Borneo Journal of Pharmacy
Vol 9 Issue 2 June 2026
Pages 153 – 164

https://journal.umpr.ac.id/index.php/bjop/article/view/10849
DOI: https://doi.org/10.33084/bjop.v9i2.10849
e-ISSN: 2621-4814

Research Article

The Effect of Thymoquinone on Progressive Brain Damage: An Experimental Study in a Wistar Rat Model of Intracerebral Hemorrhage

Khamim Thohari [1,2]

Asra Al Fauzi [3*]

Djoko Agus Purwanto [4]

[1] Doctoral Program of Medical Science, Universitas Airlangga, Surabaya, East Java, Indonesia
[2] School of Medicine, Universitas Ciputra, Surabaya, East Java, Indonesia
[3] Department of Neurosurgery, Universitas Airlangga, Surabaya, East Java, Indonesia
[4] Department of Pharmaceutical Sciences, Universitas Airlangga, Surabaya, East Java, Indonesia

*email: asra.al@fk.unair.ac.id; phone: +6281333934999

Keywords:
Inflammatory
Intracerebral hemorrhage
MMP-9
Free radicals
Thymoquinone

Abstract

Intracerebral hemorrhage (ICH) accounts for 20% of stroke cases and is associated with a 40–50% mortality rate, yet effective neuroprotective therapies remain lacking. This study evaluated the therapeutic efficacy and molecular mechanisms of thymoquinone (TQ), the primary bioactive constituent of *Nigella sativa*, in a Wistar rat model of ICH. Male Wistar rats (n = 55, 200–220 g) were randomized into five groups: untreated control, untreated ICH, vehicle-treated ICH (corn oil for 7 days), and ICH treated orally with TQ at 150 mg/kg or 250 mg/kg body weight daily for 7 days. ICH was induced via autologous blood injection (0.12 mL) into the brain parenchyma. Biomarkers for neuroinflammation (NLRP3, TNF-α, IL-6, IL-1β), oxidative stress (SOD, MDA), tissue remodeling (MMP-9), and neuronal necrosis were quantified using ELISA, immunohistochemistry, and histological staining. TQ administration significantly elevated MMP-9 levels ($p = 0.000$) compared with untreated ICH controls and markedly suppressed NLRP3, TNF-α, and IL-1β expression. Furthermore, TQ increased SOD antioxidant activity, whereas MDA levels remained elevated. These neuroprotective effects were dose-dependent, with maximal modulation observed at 250 mg/kg TQ. In conclusion, TQ modulates critical inflammatory and oxidative pathways in experimental ICH while unexpectedly upregulating MMP-9, suggesting a complex dual function in early neuroprotection and subsequent tissue remodeling. These findings demonstrate that TQ holds promising potential as a natural neuroprotective agent for hemorrhagic stroke management.

Received: September 12th, 2025
1st Revised: November 1st, 2025
2nd April: April 9th, 2026
Accepted: June 17th, 2026
Published: June 30th, 2026

INTRODUCTION

Intracerebral hemorrhage (ICH) represents one of the most devastating stroke subtypes, carrying a 40–50% mortality rate and accounting for approximately 20% of all stroke cases globally[1]. The incidence of ICH is estimated at 29.9 per 100,000 person-years, with a higher prevalence among Asian populations, males, older adults, and individuals with uncontrolled hypertension[2]. While overall stroke incidence has declined since 1990 due to improved risk factor management, stroke rates among younger adults have steadily risen since 2005[3]. In Indonesia, stroke remains a major public health crisis, generating approximately 500,000 new cases annually, with 25% leading to early mortality and a large proportion of survivors sustaining chronic disability[4]. Hemorrhagic stroke accounts for 10–15% of total stroke presentations in Indonesia, with an annual incidence of 24.6 per 100,000 individuals[5].

How to cite: Thohari K, Fauzi AA, Purwanto DA. The Effect of Thymoquinone on Progressive Brain Damage: An Experimental Study in a Wistar Rat Model of Intracerebral Hemorrhage. Borneo J Pharm. 2026;9(2):153-64. doi:10.33084/bjop.v9i2.10849

Following the primary hemorrhagic insult, secondary brain injury develops through an intricate cascade of neuroinflammatory and oxidative processes. Extravasated erythrocytes undergo lysis, releasing hemoglobin degradation products such as heme and free iron that exert direct neurotoxic effects and generate excess reactive oxygen species (ROS)[6]. Activated resident microglia and infiltrating neutrophils further exacerbate secondary damage by secreting key pro-inflammatory cytokines, including TNF-α, IL-1β, IL-6, and IL-8. These inflammatory mediators drive disruption of the blood-brain barrier, largely via transcriptional and post-translational upregulation of matrix metalloproteinase-9 (MMP-9)[7]. Concurrently, accumulated iron metabolites accelerate lipid peroxidation, trigger mitochondrial dysfunction, and induce progressive neuronal cell death[8]. Consequently, targeting neuroinflammation, oxidative stress pathways, and blood-brain barrier disintegration represents a critical therapeutic strategy in ICH management.

Despite the urgent clinical demand, current neuroprotective options for ICH remain inadequate. Conventional neuroprotective agents, including citicoline and piracetam, are used clinically but have not demonstrated satisfactory efficacy in halting progressive tissue damage or improving long-term functional recovery[9]. Hence, identifying novel therapeutic compounds that simultaneously modulate inflammatory and oxidative cascades is essential. Thymoquinone (TQ), the primary bioactive phytochemical derived from *Nigella sativa*, has emerged as a promising natural candidate possessing robust anti-inflammatory and antioxidant properties. Experimental studies indicate that TQ suppresses inflammatory signaling by inhibiting NLRP3 inflammasome activation and the NF-κB pathway, downregulating pro-inflammatory cytokine production, and reducing oxidative damage through decreased lipid peroxidation and enhanced antioxidant enzyme capacity[10-13]. These bioactivities highlight the therapeutic relevance of TQ in stroke states characterized by intense secondary neuroinflammation and vascular permeability.

In a prior experimental model of ICH in Wistar rats, TQ demonstrated significant dose-dependent neuroprotective effects, attenuating TNF-α expression, increasing NeuN-positive neuronal density, and upregulating regenerative markers such as Ki-67 and PPARγ, with 250 mg/kg showing the greatest therapeutic efficacy[14]. However, that initial investigation focused primarily on TNF-α suppression, short-term neuronal survival, and specific regenerative parameters. Critical upstream and downstream inflammatory and oxidative pathways controlling progressive secondary brain damage, specifically NLRP3, IL-1β, MMP-9, superoxide dismutase (SOD), and malondialdehyde (MDA)[15], were not evaluated. Therefore, the current investigation was conducted to systematically evaluate the therapeutic impact of TQ on secondary brain injury markers (NLRP3, TNF-α, IL-1β, MMP-9, SOD, and MDA) in a Wistar rat model of ICH, providing comprehensive mechanistic insights into its broader neuroprotective profile.

MATERIALS AND METHODS

Materials

Thymoquinone with a certified purity of ≥98% was purchased from Santa Cruz Biotechnology Inc. (Dallas, TX, USA) and solubilized in pharmaceutical-grade corn oil prior to administration. Surgical anesthesia was induced using ketamine hydrochloride, while surgical site preparation utilized povidone-iodine and 70% ethanol. Target protein and oxidative marker levels in serum were quantified using rat-specific commercial enzyme-linked immunosorbent assay (ELISA) kits, including the Rat NLRP3 ELISA Kit (REED BIOTECH, Cat. No. RE3548R-48T), Rat TNF-α ELISA Kit (REED BIOTECH, Cat. No. RE1060R), Rat IL-1β ELISA Kit (REED BIOTECH, Cat. No. RE1074R-48T), Rat MMP-9 ELISA Kit (REED BIOTECH, Cat. No. RE2796R-48T), Rat SOD1 ELISA Kit (REED BIOTECH, Cat. No. RE1626R-48T), and Rat Malondialdehyde ELISA Kit (BT LAB, Cat. No. E0156Ra-48T). For immunohistochemical evaluations, primary antibodies included anti-malondialdehyde antibody (Antibodies.com, Cambridge, UK; Cat. No. A82233) and anti-SOD1 antibody (Santa Cruz Biotechnology, Dallas, TX, USA; Cat. No. sc-1011523), along with primary antibodies for NLRP3, TNF-α, IL-1β, and MMP-9. Tissue processing and visualization reagents included 10% neutral-buffered formalin, paraffin wax, citrate antigen retrieval buffer (pH 6.0), 3% hydrogen peroxide, biotinylated secondary antibodies, streptavidin-horseradish peroxidase (HRP), 3,3'-diaminobenzidine (DAB) chromogen, and hematoxylin and eosin (H&E) counterstains. Statistical processing was performed using IBM SPSS Statistics.

Methods

Study design, setting, and ethical approval

This investigation employed a true experimental posttest-only control group design over an 8-month period from 2024 to 2025. Animal handling, housing, and experimental ICH modeling were conducted at the Biochemistry Laboratory, Faculty of Medicine, Universitas Airlangga, Surabaya, Indonesia. ELISA evaluations were performed at the Clinical Pathology Laboratory, Dr. Soetomo General Academic Hospital, Surabaya, Indonesia. Histological and immunohistochemical analyses were carried out at the Anatomical Pathology Laboratory, Faculty of Medicine, Universitas Airlangga, Surabaya, Indonesia. All experimental protocols were reviewed and approved by the Animal Care and Use Committee, Faculty of Veterinary Medicine, Universitas Airlangga (Certificate No. 2.KEH.107.07.2024; approved July 24th, 2024) in strict compliance with national and institutional guidelines for the humane care and use of laboratory animals.

Experimental animals and randomization

Healthy male Wistar rats (*Rattus norvegicus*), aged 4 months and weighing between 200 and 220 g, were selected for this study. Prior to the initiation of experiments, all animals underwent a 7-day acclimatization period under standardized laboratory conditions with free access to food and water. A total of 55 rats were randomly assigned to five experimental groups (n = 11 per group): Group P0 (normal control without ICH induction), Group P1 (ICH induction terminated at 3 hours post-insult), Group P2 (ICH induction followed by vehicle corn oil administration for 7 days), Group P3 (ICH induction followed by TQ at 150 mg/kg/day orally for 7 days), and Group P4 (ICH induction followed by TQ at 250 mg/kg/day orally for 7 days). Surgical operators and downstream histological/biochemical outcome assessors were blinded to group allocations throughout the study. The sample size was calculated using the standard formula for comparing two independent means, $n = S^2(Z\alpha + Z\beta)^2/(X_1 - X_2)^2$, yielding a minimum requirement of 9 animals per group. To account for potential dropouts during surgical induction or treatment, a 20% sample buffer was added, resulting in 11 rats per group (n = 55 total).

Thymoquinone preparation and dosing schedule

Thymoquinone was solubilized in pharmaceutical-grade corn oil as a neutral vehicle immediately before administration. Thymoquinone was delivered once daily via intragastric gavage at doses of 150 mg/kg/day (Group P3) or 250 mg/kg/day (Group P4) for 7 consecutive days following ICH induction. Animals in the vehicle control group (Group P2) received volume-matched corn oil via the same route and on the same daily schedule.

Induction of intracerebral hemorrhage

Intracerebral hemorrhage was induced using an autologous blood stereotaxic injection technique. Rats were deeply anesthetized with intraperitoneal ketamine (80–100 mg/kg). The scalp was shaved and disinfected with povidone-iodine, then with 70% ethanol. A midline scalp incision was made to expose the cranial sutures and identify the bregma and lambda landmarks. A micro-burr hole was positioned 2.5 mm lateral to the sagittal suture relative to bregma. Autologous non-anticoagulated blood was harvested from the lateral tail vein using a 23G needle into a 1 mL syringe. A total volume of 0.12 mL of autologous blood was stereotaxically injected into the striatal brain parenchyma through the designated cranial coordinate at a controlled rate of 0.02 mL/min. Following completion of the infusion, the needle was left *in situ* for 10 minutes to prevent hematoma reflux before being slowly withdrawn. The surgical site was compressed for 1 minute, sutured, and the animals were monitored in temperature-controlled recovery cages until full recovery from anesthesia.

Tissue collection and sample processing

At designated post-induction time points (3 hours for P1; 7 days for P0, P2, P3, and P4), animals were deeply anesthetized prior to terminal sacrifice. Blood was drawn via cardiac puncture into non-anticoagulated tubes, and brain tissues were harvested immediately following decapitation. Harvested brain specimens were immersion-fixed in 10% neutral buffered formalin for downstream histological and immunohistochemical evaluation. Whole blood samples were centrifuged to separate serum, which was aliquoted and stored at -20 °C until ELISA quantification.

Enzyme-linked immunosorbent assay

Serum concentrations of NLRP3, TNF-α, IL-1β, MMP-9, SOD, and MDA were quantified using rat-specific commercial ELISA kits according to the manufacturers' precise instructions. The specific assay kits utilized were: Rat NLRP3 ELISA Kit, Rat TNF-α ELISA Kit, Rat IL-1β ELISA Kit, Rat MMP-9 ELISA Kit, Rat SOD1 ELISA Kit, and Rat MDA ELISA Kit. Briefly, standard solutions and serum samples were added to microplate wells pre-coated with target-specific antibodies, incubated, washed, and reacted with HRP-conjugated detection reagents and tetramethylbenzidine (TMB) substrate solution. Absorbance was read at 450 nm using an automated microplate spectrophotometer, and target protein concentrations were calculated against standard curves.

Immunohistochemical analysis

Formalin-fixed brain specimens were embedded in paraffin blocks and sectioned at a thickness of 4 um. Tissue sections were deparaffinized in xylene, rehydrated through a graded ethanol series, and subjected to heat-induced epitope retrieval in citrate buffer (pH 6.0). Endogenous peroxidase activity was quenched using 3% hydrogen peroxide, followed by incubation with background-blocking serum. Sections were incubated overnight with primary antibodies targeting NLRP3, TNF-α, IL-1β, MMP-9, MDA, and SOD1. Immunoreactivity was visualized using a biotinylated secondary antibody, streptavidin-HRP, and DAB chromogen, followed by hematoxylin counterstaining.

Histological quantification of neuronal necrosis

Histopathological damage was evaluated on paraffin sections stained with H&E. Stained brain sections were examined under a light microscope at 400x magnification. Neuronal necrosis was morphologically identified by characteristic nuclear pyknosis, karyorrhexis, karyolysis, and cytoplasmic eosinophilia with membrane blebbing. The number of necrotic neurons was systematically counted across high-power fields (HPFs) within the peri-hematomal region.

Data analysis

Data were summarized using descriptive statistics and presented as mean ± standard deviation or median with minimum–maximum ranges, depending on the distribution characteristics. Normality of data within each experimental group was formally tested using the Shapiro–Wilk test, selected given the sample size of 11 rats per group. Because biological parameters exhibited non-normal distributions, non-parametric statistical methods were employed. Differences across the five treatment groups were evaluated using the Kruskal–Wallis test. Upon detecting statistically significant differences among groups, post-hoc pairwise comparisons were conducted using the Mann–Whitney U test. Statistical significance was defined as a two-tailed p-value <0.05. All statistical computations were performed using IBM SPSS Statistics software.

RESULTS AND DISCUSSION

Descriptive statistical profiles for NLRP3, TNF-α, MMP-9, IL-1β, SOD, and MDA across all experimental groups are detailed in **Tables I** to **VI** and illustrated in **Figures 1** to **6**. Biomarker responses exhibited noticeable intergroup variations without demonstrating a uniform dose-dependent pattern across all measured parameters. NLRP3 levels are presented in **Table I** and **Figure 1**. Median NLRP3 values were recorded at 0.555 in the control group, 0.185 in the ICH 3-hour group, and 0.450 in the untreated ICH 7-day group. Following TQ administration, median NLRP3 concentrations decreased to 0.315 in the TQ 150 mg/kg group and 0.293 in the TQ 250 mg/kg group. Although median values in the TQ-treated cohorts were lower than those in the ICH 7-day untreated control, wide data ranges (particularly within the ICH 7-day and TQ 250 mg/kg groups) highlighted substantial inter-individual variability in NLRP3 response.

Table I. Descriptive statistics for NLRP3 across experimental groups.

Parameter	Grouping	Minimum	Maximum	Median	Mean ± SD
NLRP3	Control	0.279	0.868	0.555	0.576 ± 0.192
	ICH 3 Hours	0.069	0.872	0.185	0.287 ± 0.222
	ICH 7 Days	0.005	4.150	0.450	0.729 ± 1.102
	ICH + TQ 150 mg	0.004	0.912	0.315	0.383 ± 0.324
	ICH + TQ 250 mg	0.059	2.608	0.293	0.581 ± 0.731

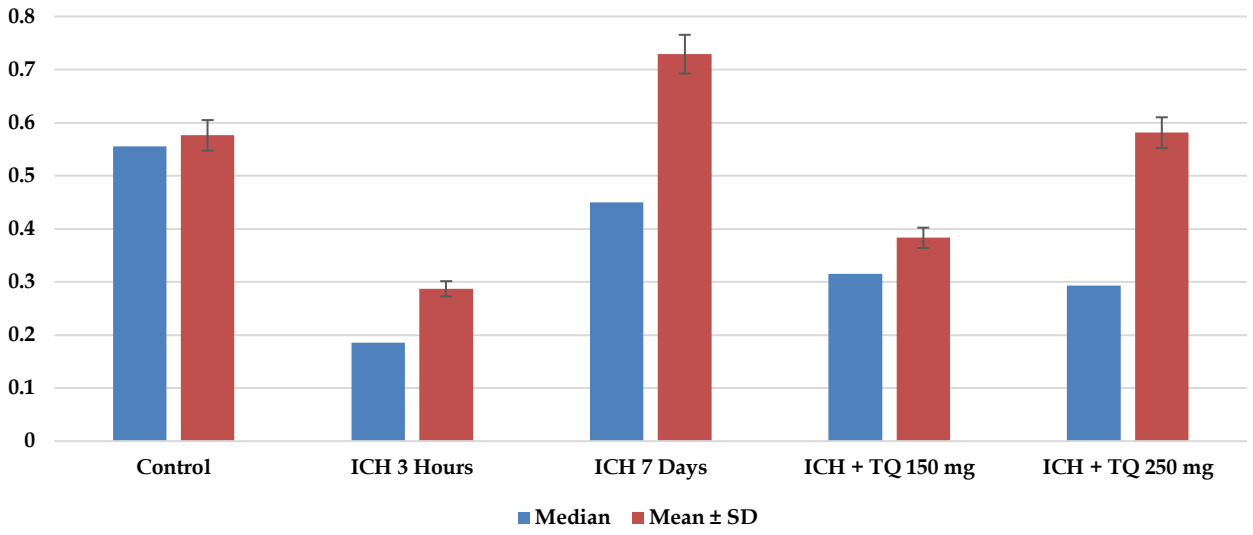

Figure 1. Comparison of serum NLRP3 expression across experimental groups.

TNF-α levels are detailed in **Table II** and **Figure 2**. The median TNF-α concentration was 2.906 in the control group, rising slightly to 3.072 in the acute ICH 3-hour group before falling to 1.887 by day 7. In TQ-treated animals, median TNF-α values were 2.879 in the 150 mg/kg group and 1.728 in the 250 mg/kg group. These data indicate a downward trend at the higher therapeutic dose, though the high standard deviation in the 250 mg/kg group warrants cautious interpretation[16].
MMP-9 concentrations are shown in **Table III** and **Figure 3**. Median MMP-9 levels were 472.67 in controls, increased to 598.50 at 3 hours post-ICH, and returned to 467.54 at 7 days. Conversely, TQ administration increased MMP-9 expression, with median values of 782.05 in the TQ 150 mg/kg group and 795.01 in the TQ 250 mg/kg group, indicating a consistent post-treatment increase relative to untreated controls.

Table II. Descriptive statistics for TNF-α across experimental groups.

Parameter	Grouping	Minimum	Maximum	Median	Mean ± SD
TNF-α	Control	2.232	4.427	2.906	2.997 ± 0.726
	ICH 3 Hours	1.738	7.200	3.072	3.325 ± 1.646
	ICH 7 Days	1.415	4.844	1.887	2.287 ± 1.087
	ICH + TQ 150 mg	2.028	4.844	2.879	3.029 ± 0.921
	ICH + TQ 250 mg	0.987	12.996	1.728	3.877 ± 3.887

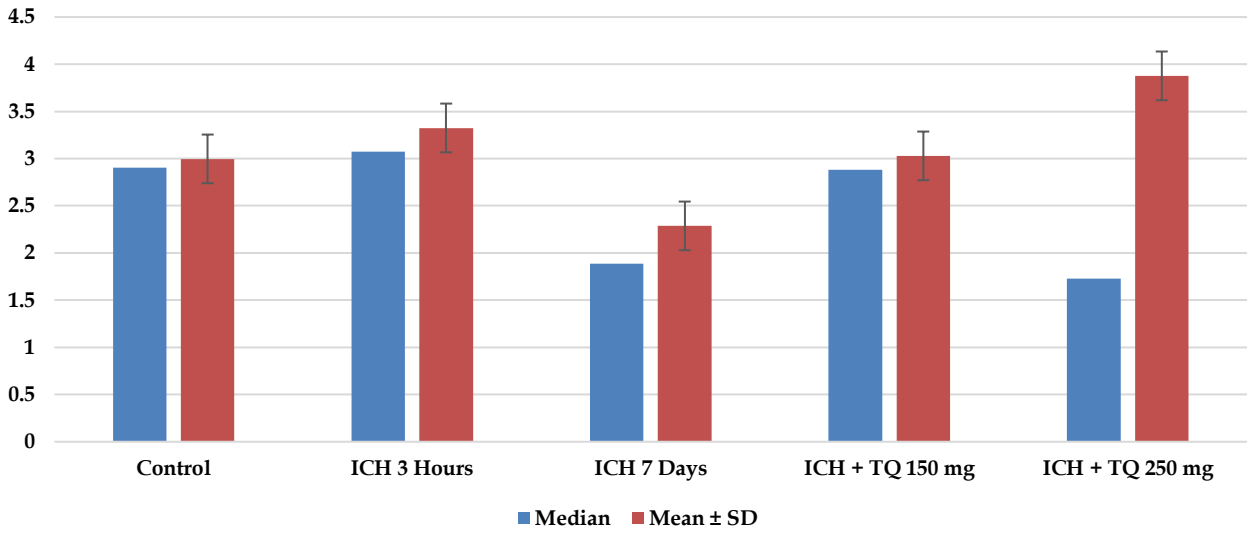

Figure 2. Comparison of serum TNF-α expression across experimental groups.

Table III. Descriptive statistics for MMP-9 across experimental groups.

Parameter	Grouping	Minimum	Maximum	Median	Mean ± SD
MMP-9	Control	310.41	598.94	472.67	479.41 ± 96.38
	ICH 3 Hours	320.63	899.23	598.50	598.54 ± 188.69
	ICH 7 Days	347.90	773.32	467.54	485.96 ± 112.97
	ICH + TQ 150 mg	504.50	1001.43	782.05	779.34 ± 135.19
	ICH + TQ 250 mg	426.48	1119.04	795.01	828.22 ± 263.94

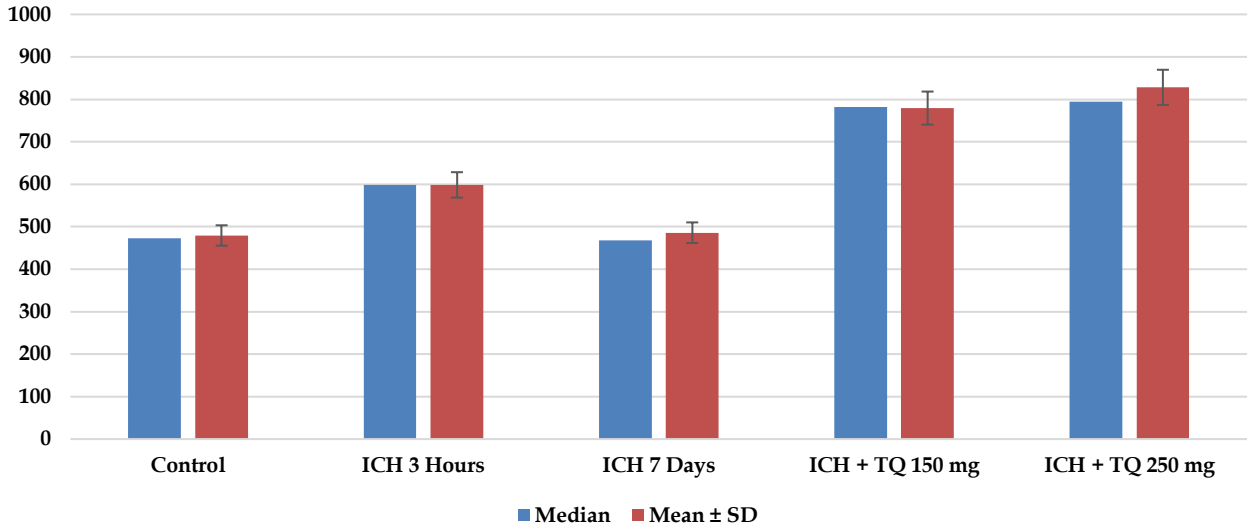

Figure 3. Comparison of serum MMP-9 expression across experimental groups.

IL-1β profile parameters are summarized in **Table IV** and **Figure 4**. Median IL-1β concentrations measured 3.604 in the control group, 2.210 in the ICH 3-hour group, and 3.755 in the ICH 7-day group. Thymoquinone treatment produced median values of 2.333 at 150 mg/kg and 2.129 at 250 mg/kg. While median levels were lower following treatment, extreme variance in the TQ 250 mg/kg cohort (standard deviation exceeding the mean) indicates a descriptive trend rather than a definitive effect. SOD antioxidant levels are reported in **Table V** and **Figure 5**. Median SOD levels measured 393.30 in controls, 367.77 in the ICH 3-hour group, and 468.96 in the ICH 7-day group. In the TQ-treated groups, the median values were 400.72 (150 mg/kg) and 353.94 (250 mg/kg). These results demonstrate fluctuating SOD concentrations without a clear dose-dependent trajectory. MDA lipid peroxidation profiles are presented in **Table VI** and **Figure 6**. Median MDA was 305.41 in controls, rising to 348.14 at 3 hours and 388.91 at 7 days post-ICH. Thymoquinone treatment maintained elevated median levels of 427.22 (150 mg/kg) and 399.85 (250 mg/kg), indicating that TQ did not consistently lower serum lipid peroxidation across these observation windows[17].

Results of the Shapiro–Wilk test for normality are compiled in **Table VII**. Several markers exhibited significant non-normality in specific experimental groups, including NLRP3, TNF-α, MMP-9, IL-1β, and MDA ($p < 0.05$). Conversely, SOD maintained a normal distribution across all study groups. Given these distributional properties and the modest sample sizes per group, non-parametric analytical methods were adopted for hypothesis testing[18]. Group comparisons, evaluated using the Kruskal–Wallis test (**Table VIII**), identified MMP-9 as the only biomarker showing a statistically significant intergroup difference ($H = 25.174$, $p < 0.001$). Differences across groups for TNF-α ($p = 0.130$), NLRP3 ($p = 0.127$), IL-1β ($p = 0.518$), SOD ($p = 0.232$), and MDA ($p = 0.064$) did not reach statistical significance and are interpreted as descriptive trends.

Table IV. Descriptive statistics for IL-1β across experimental groups.

Parameter	Grouping	Minimum	Maximum	Median	Mean ± SD
IL-1β	Control	-1.065	16.601	3.604	4.901 ± 4.949
	ICH 3 Hours	0.490	4.474	2.210	2.362 ± 1.438
	ICH 7 Days	1.102	9.085	3.755	4.011 ± 2.665
	ICH + TQ 150 mg	1.480	7.233	2.333	3.199 ± 1.947
	ICH + TQ 250 mg	0.154	52.573	2.129	7.183 ± 16.024

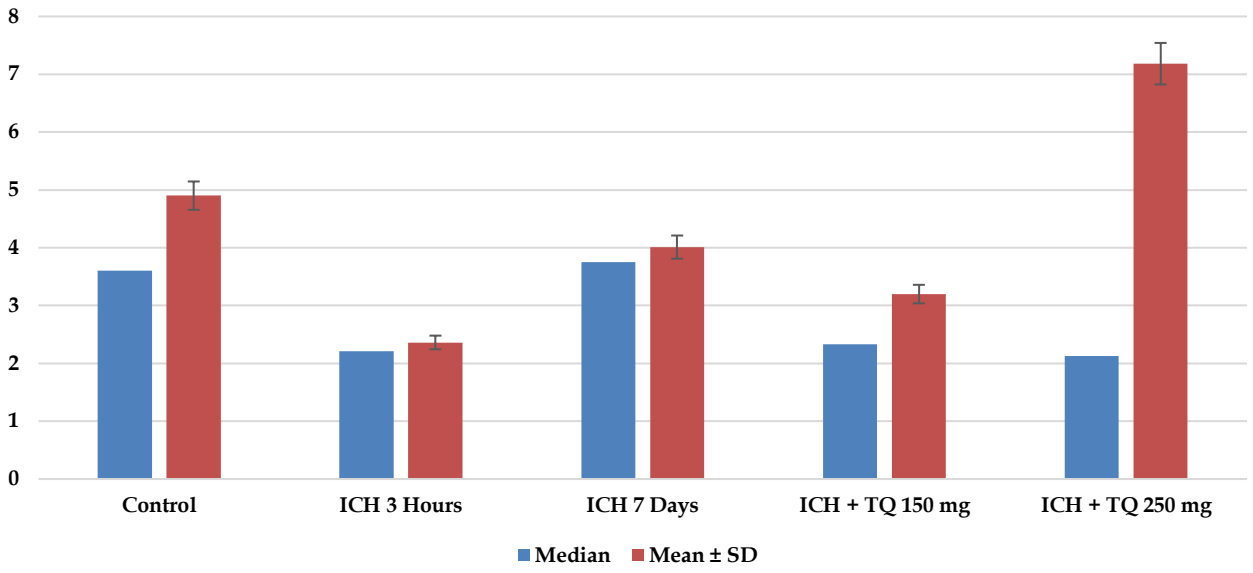

Figure 4. Comparison of serum IL-1β expression across experimental groups.

Table V. Descriptive statistics for SOD across experimental groups.

Parameter	Grouping	Minimum	Maximum	Median	Mean ± SD
SOD	Control	306.94	519.75	393.30	389.18 ± 71.31
	ICH 3 Hours	312.56	543.02	367.77	406.18 ± 80.36
	ICH 7 Days	328.21	546.65	468.96	454.01 ± 75.73
	ICH + TQ 150 mg	214.86	551.97	400.72	421.46 ± 109.25
	ICH + TQ 250 mg	141.74	600.76	353.94	356.72 ± 112.03

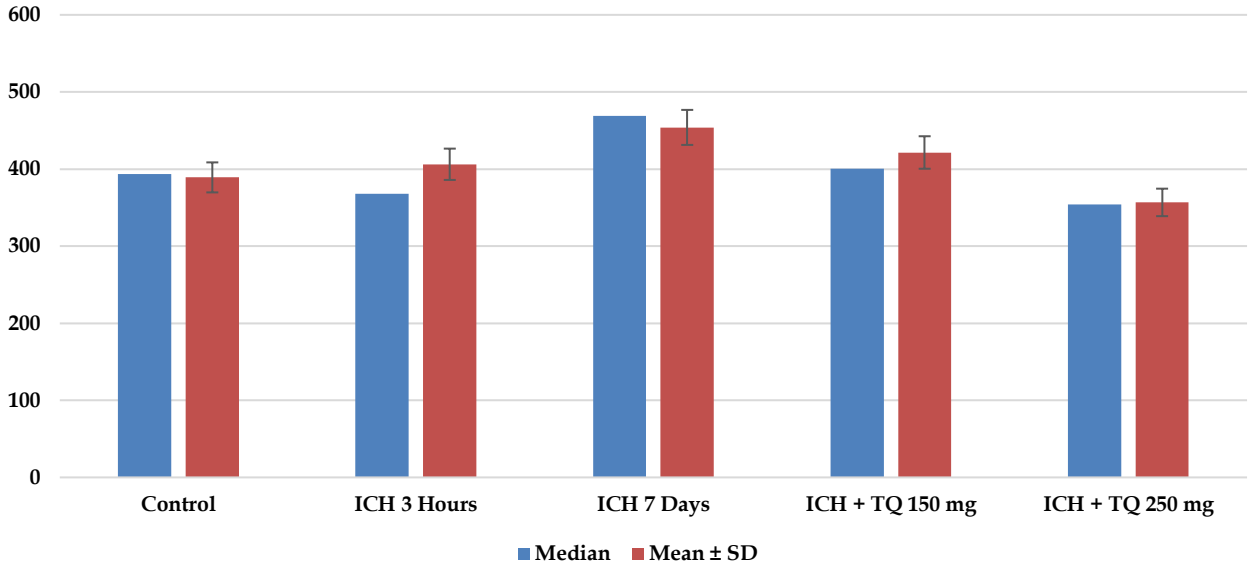

Figure 5. Comparison of serum SOD expression across experimental groups.

Table VI. Descriptive statistics for MDA across experimental groups.

Parameter	Grouping	Minimum	Maximum	Median	Mean ± SD
MDA	Control	259.18	645.25	305.41	356.22 ± 119.57
	ICH 3 Hours	272.06	533.72	348.14	371.90 ± 75.39
	ICH 7 Days	262.18	825.54	388.91	440.75 ± 155.42
	ICH + TQ 150 mg	351.66	1037.92	427.22	507.38 ± 202.07
	ICH + TQ 250 mg	280.99	520.69	399.85	392.46 ± 72.42

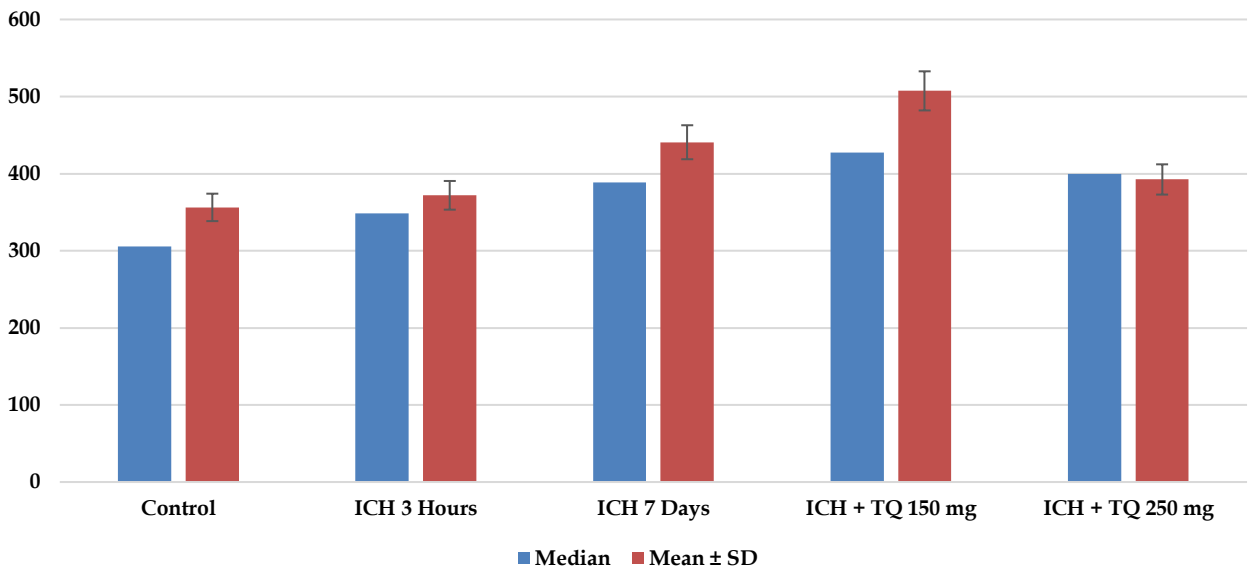

Figure 6. Comparison of serum MDA expression across experimental groups.

Table VII. Shapiro–Wilk normality test results for inflammatory and oxidative biomarkers.

Parameter	Grouping	Shapiro–Wilk Statistic	p-value	Distribution Assessment
TNF-α	Control	0.903	0.239	Normal
	ICH 3 Hours	0.860	0.058	Normal
	ICH 7 Days	0.782	0.013	Abnormal
	ICH + TQ 150 mg	0.874	0.086	Normal
	ICH + TQ 250 mg	0.955	0.749	Normal
NLRP3	Control	0.960	0.766	Normal
	ICH 3 Hours	0.780	0.005	Abnormal
	ICH 7 Days	0.530	0.000	Abnormal
	ICH + TQ 150 mg	0.919	0.307	Normal
	ICH + TQ 250 mg	0.697	0.001	Abnormal
MMP-9	Control	0.937	0.520	Normal
	ICH 3 Hours	0.954	0.696	Normal
	ICH 7 Days	0.845	0.037	Abnormal
	ICH + TQ 150 mg	0.980	0.964	Normal
	ICH + TQ 250 mg	0.840	0.045	Abnormal
IL-1β	Control	0.858	0.073	Normal
	ICH 3 Hours	0.924	0.350	Normal
	ICH 7 Days	0.902	0.233	Normal
	ICH + TQ 150 mg	0.792	0.012	Abnormal
	ICH + TQ 250 mg	0.454	0.000	Abnormal
SOD	Control	0.921	0.330	Normal
	ICH 3 Hours	0.889	0.136	Normal
	ICH 7 Days	0.907	0.225	Normal
	ICH + TQ 150 mg	0.922	0.340	Normal
	ICH + TQ 250 mg	0.912	0.255	Normal
MDA	Control	0.788	0.010	Abnormal
	ICH 3 Hours	0.896	0.230	Normal
	ICH 7 Days	0.896	0.230	Normal
	ICH + TQ 150 mg	0.708	0.001	Abnormal
	ICH + TQ 250 mg	0.716	0.001	Abnormal

Post hoc pairwise Mann–Whitney U testing (**Table IX**) confirmed significant increases in MMP-9 between controls and both the TQ 150 mg/kg ($p = 0.003$) and TQ 250 mg/kg ($p = 0.011$) groups. MMP-9 levels in the untreated 7-day ICH group also differed significantly from the TQ 150 mg/kg ($p = 0.001$) and TQ 250 mg/kg ($p = 0.005$) cohorts. The difference between the 3-hour ICH group and the TQ 150 mg/kg group was statistically significant ($p = 0.020$), whereas the comparison with the TQ 250 mg/kg group approached significance ($p = 0.057$). Overall, TQ administration significantly increased serum MMP-9 levels while other inflammatory and oxidative markers demonstrated variable, non-significant trends.

Table VIII. Statistical analysis of biomarkers via the Kruskal–Wallis test.

Parameter	Grouping	Median	Mean ± SD	Kruskal–Wallis H (p-value)	Analytical Conclusion
TNF-α	Control	2.906	2.997 ± 0.726	8.509 (0.130)	No Meaningful Difference
	ICH 3 Hours	3.072	3.325 ± 1.646		
	ICH 7 Days	1.887	2.287 ± 1.087		
	ICH + TQ 150 mg	2.879	3.029 ± 0.921		
	ICH + TQ 250 mg	2.140	2.217 ± 0.476		
NLRP3	Control	0.555	0.576 ± 0.192	8.591 (0.127)	No Meaningful Difference
	ICH 3 Hours	0.185	0.287 ± 0.222		
	ICH 7 Days	0.450	0.729 ± 1.102		
	ICH + TQ 150 mg	0.315	0.383 ± 0.324		
	ICH + TQ 250 mg	0.293	0.581 ± 0.731		
MMP-9	Control	472.67	479.41 ± 96.38	25.174 (<0.001)	Meaningful Difference
	ICH 3 Hours	598.50	598.54 ± 188.69		
	ICH 7 Days	467.54	485.96 ± 112.97		
	ICH + TQ 150 mg	782.05	779.34 ± 135.19		
	ICH + TQ 250 mg	764.77	838.45 ± 334.66		
IL-1β	Control	3.755	4.011 ± 2.665	4.219 (0.518)	No Meaningful Difference
	ICH 3 Hours	2.333	3.199 ± 1.947		
	ICH 7 Days	2.210	2.362 ± 1.438		
	ICH + TQ 150 mg	2.386	3.097 ± 2.021		
	ICH + TQ 250 mg	393.30	389.18 ± 71.31		
SOD	Control	468.96	454.01 ± 75.73	6.853 (0.232)	No Meaningful Difference
	ICH 3 Hours	400.72	421.46 ± 109.25		
	ICH 7 Days	367.77	406.18 ± 80.36		
	ICH + TQ 150 mg	353.94	356.72 ± 112.03		
	ICH + TQ 250 mg	305.41	356.22 ± 119.57		
MDA	Control	388.91	440.75 ± 155.42	10.433 (0.064)	No Meaningful Difference
	ICH 3 Hours	427.22	507.38 ± 202.07		
	ICH 7 Days	348.14	371.90 ± 75.39		
	ICH + TQ 150 mg	399.85	392.46 ± 72.42		
	ICH + TQ 250 mg	305.41	356.22 ± 119.57		

Table IX. Post-Hoc pairwise Mann–Whitney U analysis of MMP-9 expression.

Baseline Group	Baseline Median	ICH Day 7 + TQ 150 mg (U-statistic; p-value)	ICH Day 7 + TQ 250 mg (U-statistic; p-value)
Control	502.03	15.000 (p = 0.003)	19.000 (p = 0.011)
ICH 3 Hours	598.50	25.000 (p = 0.020)	28.000 (p = 0.057)
ICH Day 7	467.54	8.000 (p = 0.001)	15.000 (p = 0.005)
ICH Day 7 + TQ 150 mg	782.05	—	—
ICH Day 7 + TQ 250 mg	764.77	—	—

The present study evaluated the systemic modulation of neuroinflammatory and oxidative stress markers following TQ administration in a rat model of ICH. Inferential analysis revealed that TQ significantly affected serum MMP-9 levels, whereas NLRP3, TNF-α, IL-1β, SOD, and MDA displayed variable, non-significant trends. As confirmed by Kruskal–Wallis testing, MMP-9 was the sole parameter to exhibit significant intergroup variance ($p < 0.001$), establishing it as the primary biomarker of treatment response in this experimental model.

MMP-9 levels rose from 472.67 in controls to 598.50 at 3 hours post-ICH, then returned to baseline (467.54) by day 7 in untreated animals. Conversely, TQ treatment markedly elevated median MMP-9 expression to 782.05 at 150 mg/kg and 795.01 at 250 mg/kg. Post hoc pairwise comparisons confirmed significant elevations relative to both 7-day untreated controls ($p=0.001$ for 150 mg/kg; $p=0.005$ for 250 mg/kg) and healthy controls ($p=0.003$ for 150 mg/kg; $p=0.011$ for 250 mg/kg). While acute MMP-9 upregulation traditionally promotes blood–brain barrier breakdown and neuroinflammation[14,19,20], matrix metalloproteinases display distinct phase-dependent roles after stroke. During the subacute and chronic repair phases, elevated MMP-9 levels contribute to extracellular matrix reorganization, neurovascular remodeling, and angiogenesis[21]. The sustained elevation of MMP-9 observed at day 7 in TQ-treated animals suggests a functional shift toward tissue remodeling and recovery rather than acute pathological breakdown, supporting a time-dependent mechanism for TQ in central nervous system injury[9,22].

In contrast, inflammatory markers (NLRP3, TNF-α, and IL-1β) showed non-significant declines following TQ administration. Median NLRP3 values decreased from 0.450 in the 7-day ICH group to 0.315 (150 mg/kg TQ) and 0.293 (250 mg/kg TQ), while TNF-α and IL-1β also exhibited reductions at high doses. These trends align with established reports

that TQ attenuates neuroinflammation by suppressing NF-κB and NLRP3 inflammasome signaling pathways[12]. However, high variance and wide standard deviations indicate substantial biological heterogeneity in autologous blood models. Moreover, because post-ICH cytokine cascades typically peak within 24–72 hours, sampling at 3 hours and 7 days may have omitted the peak inflammatory window, accounting for the lack of statistical significance.

Oxidative stress responses similarly exhibited non-significant shifts. Median SOD levels fluctuated across groups without a clear dose-response relationship, and MDA levels remained elevated in TQ-treated cohorts. Although TQ activates Nrf2-driven antioxidant defenses in other experimental models[23,24], 7 days of treatment did not significantly lower lipid peroxidation in this setting. This suggests that while endogenous antioxidant pathways may be engaged, ROS generation following hemoglobin degradation persists beyond 7 days. These findings demonstrate that the therapeutic effects of TQ in ICH are marker-specific and phase-dependent[25], highlighting the need for multi-timepoint sampling across acute and subacute phases to further clarify its therapeutic scope.

CONCLUSION

Thymoquinone administration significantly modulated MMP-9 expression in a Wistar rat model of ICH, with a marked upregulation in TQ-treated groups compared with untreated post-ICH controls. In contrast, key inflammatory mediators (NLRP3, TNF-α, and IL-1β) showed a general downward trend, while oxidative stress indicators (SOD and MDA) showed variable, non-linear responses; however, these changes in secondary parameters were not statistically significant. Collectively, these findings indicate that the biological effects of TQ on post-ICH neuroinflammatory and oxidative pathways are complex, marker-specific, and time-dependent. Rather than reflecting acute pathological damage alone, the sustained elevation of MMP-9 at day 7 post-insult suggests a potential dual, phase-dependent role involving subacute extracellular matrix remodeling and neurovascular repair. Nevertheless, the precise contribution of elevated MMP-9 to either injury progression or tissue remodeling remains hypothetical and warrants rigorous mechanistic validation. To clarify the temporal kinetics of post-hemorrhagic inflammation, oxidative stress, and MMP-9 activity, and to pinpoint the optimal therapeutic window for TQ, future studies incorporating expanded early-phase observation points, particularly on days 1 and 3 post-ICH, are strongly recommended.

ACKNOWLEDGMENT

None.

AUTHORS' CONTRIBUTION

Conceptualization: Khamim Thohari, Asra Al Fauzi
Data curation: Khamim Thohari
Formal analysis: Khamim Thohari
Funding acquisition: -
Investigation: Khamim Thohari
Methodology: Khamim Thohari, Asra Al Fauzi
Project administration: Khamim Thohari
Resources: Khamim Thohari, Asra Al Fauzi
Software: -
Supervision: Asra Al Fauzi, Djoko Agus Purwanto
Validation: Asra Al Fauzi, Djoko Agus Purwanto
Visualization: Khamim Thohari
Writing - original draft: Khamim Thohari
Writing - review & editing: Khamim Thohari, Asra Al Fauzi, Djoko Agus Purwanto

DATA AVAILABILITY

None.

CONFLICT OF INTEREST

The authors declared no conflict of interest.

REFERENCES

1. Montaño A, Hanley DF, Hemphill JC 3rd. Hemorrhagic stroke. Handb Clin Neurol. 2021;176:229-48. DOI: 10.1016/B978-0-444-64034-5.00019-5; PMID: 33272397.

2. Wang S, Zou XL, Wu LX, Zhou HF, Xiao L, Yao T, et al. Epidemiology of intracerebral hemorrhage: A systematic review and meta-analysis. Front Neurol. 2022;13:915813. DOI: 10.3389/fneur.2022.915813; PMID: 36188383; PMCID: PMC9523083.

3. Lindsay MP, Norrving B, Sacco RL, Brainin M, Hacke W, Martins S, et al. World Stroke Organization (WSO): Global Stroke Fact Sheet 2019. Int J Stroke. 2019;14(8):806-17. DOI: 10.1177/1747493019881353; PMID: 31658892.

4. Yudawijaya A, Suling FRW. Comparison of hypertension risk factors in Hemorric Stroke with Non-Hemorric Stroke in UKI General Hospital, East Jakarta. Int J Med Health Res. 2022;8(3):40-8.

5. Yuniati D, Syifak S, Putra PA, Saffanah VSP. Intracerebral hemorrhage Score as a Prognosis Prediction of Spontaneous Intracerebral hemorrhage at RSI Surabaya Jemursari. AKSONA. 2023;3(2):67-73. DOI: 10.20473/aksona.v3i2.40242.

6. Shao Z, Tu S, Shao A. Pathophysiological Mechanisms and Potential Therapeutic Targets in Intracerebral Hemorrhage. Front Pharmacol. 2019;10:1079. DOI: 10.3389/fphar.2019.01079; PMID: 31607923; PMCID: PMC6761372.

7. Zheng S, Jian D, Gan H, Wang L, Zhao J, Zhai X. FUNDC1 inhibits NLRP3-mediated inflammation after intracerebral hemorrhage by promoting mitophagy in mice. Neurosci Lett. 2021;756:135967. DOI: 10.1016/j.neulet.2021.135967; PMID: 34022268.

8. Liu T, Li X, Cui Y, Meng P, Zeng G, Wang Y, Wang Q. Bioinformatics Analysis Identifies Potential Ferroptosis Key Genes in the Pathogenesis of Intracerebral Hemorrhage. Front Neurosci. 2021;15:661663. DOI: 10.3389/fnins.2021.661663; PMID: 34163322; PMCID: PMC8215678.

9. Shad KF, Soubra W, Cordato DJ. The role of thymoquinone, a major constituent of Nigella sativa, in the treatment of inflammatory and infectious diseases. Clin Exp Pharmacol Physiol. 2021;48(11):1445-53. DOI: 10.1111/1440-1681.13553; PMID: 34297870.

10. Bordoni L, Fedeli D, Nasuti C, Maggi F, Papa F, Wabitsch M, De Caterina R, Gabbianelli R. Antioxidant and Anti-Inflammatory Properties of *Nigella sativa* Oil in Human Pre-Adipocytes. Antioxidants. 2019;8(2):51. DOI: 10.3390/antiox8020051; PMID: 30823525; PMCID: PMC6406245.

11. Tadi P, Lui F. Acute Stroke. In: StatPearls. Treasure Island (FL): StatPearls Publishing; 2026. NBKID: NBK535369

12. Amartey J, Gapper S, Hussein N, Morris K, Withycombe CE. Nigella sativa extract and thymoquinone regulate inflammatory cytokine and TET-2 expression in endothelial cells. Artery Res. 2019;25(3):157-63. DOI: 10.2991/artres.k.191114.002.

13. Cobourne-Duval MK, Taka E, Mendonca P, Soliman KFA. Thymoquinone increases the expression of neuroprotective proteins while decreasing the expression of pro-inflammatory cytokines and the gene expression NFκB pathway signaling targets in LPS/IFNγ -activated BV-2 microglia cells. J Neuroimmunol. 2018;320:87-97. DOI: 10.1016/j.jneuroim.2018.04.018; PMID: 29759145; PMCID: PMC5967628.

14. Durak MA, Ozhan O, Yildiz A, Durhan M, Vardi N, Cigremis Y, et al. Protective effect of short-term thymoquinone administration on the central nervous system in cisplatin-induced neurotoxicity. Eur Rev Med Pharmacol Sci. 2022;26(19):6935-43. DOI: 10.26355/eurrev_202210_29874; PMID: 36263573.

15. Hu X, Tao C, Gan Q, Zheng J, Li H, You C. Oxidative Stress in Intracerebral Hemorrhage: Sources, Mechanisms, and Therapeutic Targets. Oxid Med Cell Longev. 2016;2016:3215391. DOI: 10.1155/2016/3215391; PMID: 26843907; PMCID: PMC4710930.

16. Zhao S, Jiang J, Jing Y, Liu W, Yang X, Hou X, et al. The concentration of tumor necrosis factor-α determines its protective or damaging effect on liver injury by regulating Yap activity. Cell Death Dis. 2020;11(1):70. DOI: 10.1038/s41419-020-2264-z; PMID: 31988281; PMCID: PMC6985193.

17. Isaev NK, Genrikhs EE, Stelmashook EV. Antioxidant Thymoquinone and Its Potential in the Treatment of Neurological Diseases. Antioxidants. 2023;12(2):433. DOI: 10.3390/antiox12020433; PMID: 36829993; PMCID: PMC9952318.

18. Liu Y, Huang L, Kim MY, Cho JY. The Role of Thymoquinone in Inflammatory Response in Chronic Diseases. Int J Mol Sci. 2022;23(18):10246. DOI: 10.3390/ijms231810246; PMID: 36142148; PMCID: PMC9499585.

19. Fanoudi S, Alavi MS, Hosseini M, Sadeghnia HR. Nigella sativa and thymoquinone attenuate oxidative stress and cognitive impairment following cerebral hypoperfusion in rats. Metab Brain Dis. 2019;34(4):1001-10. DOI: 10.1007/s11011-019-00394-4; PMID: 31016464.

20. Könnecke H, Bechmann I. The role of microglia and matrix metalloproteinases involvement in neuroinflammation and gliomas. Clin Dev Immunol. 2013;2013:914104. DOI: 10.1155/2013/914104; PMID: 24023566; PMCID: PMC3759277.

21. Guan X, Li M, Li H, Guo Z, Ullah MS, Liu X, Wu M, Yu W. The role of MMPs in intracerebral hemorrhage. Front Cell Dev Biol. 2025;13:1667228. DOI: 10.3389/fcell.2025.1667228; PMID: 41480312; PMCID: PMC12754015.

22. Kaymak E, Akin AT, Öztürk E, Karabulut D, Kuloğlu N, Yakan B. Thymoquinone has a neuroprotective effect against inflammation, oxidative stress, and endoplasmic reticulum stress in the brain cortex, medulla, and hippocampus due to doxorubicin. J Biochem Mol Toxicol. 2021;35(11):e22888. DOI: 10.1002/jbt.22888; PMID: 34392583.

23. Behairy A, Elkomy A, Elsayed F, Gaballa MMS, Soliman A, Aboubakr M. Antioxidant and anti-inflammatory potential of spirulina and thymoquinone mitigate the methotrexate-induced neurotoxicity. Naunyn Schmiedebergs Arch Pharmacol. 2024;397(3):1875-88. DOI: 10.1007/s00210-023-02739-4; PMID: 37773524; PMCID: PMC10858838.

24. Zhang Y, Yu W, Liu Y, Chang W, Wang M, Zhang L. Regulation of nuclear factor erythroid-2-related factor 2 as a potential therapeutic target in intracerebral hemorrhage. Front Mol Neurosci. 2022;15:995518. DOI: 10.3389/fnmol.2022.995518; PMID: 36245922; PMCID: PMC9559574.

25. Pottoo FH, Ibrahim AM, Alammar A, Alsinan R, Aleid M, Alshehhi A, Alshehri M, Mishra S, Alhajri N. Thymoquinone: Review of Its Potential in the Treatment of Neurological Diseases. Pharmaceuticals. 2022;15(4):408. DOI: 10.3390/ph15040408; PMID: 35455405; PMCID: PMC9026861.